Using satellite altimetry data to augment flow estimation techniques on the Mekong River

S. J. Birkinshaw,[1]* G. M. O'Donnell,[1] P. Moore,[1] C. G. Kilsby,[1] H. J. Fowler[1]
and P. A. M. Berry[2]

[1] *School of Civil Engineering and Geosciences, Newcastle University, Newcastle NE1 7RU, UK*
[2] *Earth and Planetary Remote Sensing Laboratory, De Montfort University, Leicester LE1 9BH, UK*

Abstract:

Satellite altimetry is routinely used to provide levels for oceans or large inland water bodies from space. By utilizing retracking schemes specially designed for inland waters, meaningful river stages can also be recovered when standard techniques fail. Utilizing retracked waveforms from ERS-2 and ENVISAT along the Mekong, comparisons against observed stage measurements show that the altimetric measurements have a root mean square error (RMSE) of 0·44–0·65 m for ENVISAT and 0·46–0·76 m for ERS-2. For many applications, however, stage is insufficient because discharge is the primary requirement. Investigations were therefore undertaken to estimate discharges at a downstream site (Nakhon Phanom (NP)) assuming that *in situ* data are available at a site 400 km upstream (Vientiane). Two hypothetical, but realistic scenarios were considered. Firstly, that NP was the site of a de-commissioned gauge and secondly, that the site has never been gauged. Using both scenarios, predictions were made for the daily discharge using methods with and without altimetric stage data. In the first scenario using a linear regression approach the altimetry data improved the Nash-Sutcliffe r^2 value from 0·884 to 0·935. The second scenario used known river cross-sections while lateral inflows were inferred from a hydrological model: this scenario gave an increase in the r^2 value from 0·823 to 0·893. The use of altimetric stage data is shown to improve estimated discharges and further applications are discussed. Copyright © 2010 John Wiley & Sons, Ltd.

KEY WORDS   Radar altimetry; remote sensing; discharge estimates; river velocity; rating-curve; Mekong

Received 21 July 2009; Accepted 14 June 2010

INTRODUCTION

Knowledge of the variability in river discharge is of fundamental importance to planners managing flood hazards and water resources and to scientists concerned with climate change. However, assessment of climate change impacts on hydrology is severely constrained by lack of measurements of water storage and flows at the catchment scale for use in hydrological models (Vörösmarty *et al.*, 1999). Over much of the Earth availability of *in situ* gauge data of stage (or level) and discharge has declined over the past decades. For example, there has been a 66% reduction in operational gauges since 1985 (Nijssen *et al.*, 2001) in northern latitudes while stations in the R-Arctic net 3·0 dataset declined from 1198 operating between 1960 and 1985 to just 280 operating between 1985 and 2000.

In contrast, the past decade has witnessed increased interest and capability in monitoring inland water using space borne instrumentation. In particular, the availability of satellite altimetry from ERS-2 and ENVISAT and from Jason-1 and Jason-2 is continually adding to the time series of measurements of inland water levels that started with the launch of ERS-1 in 1991 and TOPEX/Poseidon

in 1992. Water level change has also been measured using interferometric radar measurements (e.g. Alsdorf *et al.*, 2001). Other space borne instrumentation such as synthetic aperture radars, microwave radiometers and multi-temporal imagery also provide measures of water extent (Alsdorf, 2003; Bates *et al.*, 2006; Alsdorf *et al.*, 2007; Smith *et al.*, 2008).

Of the possibilities for measuring water level from space, altimetry has perhaps the greatest potential. Early results utilized the standard altimetric geophysical data records (GDR) produced primarily for oceanographic purposes but with data available over some inland rivers and lakes. For example, Birkett *et al.* (2002), Coe and Birkett (2004) and Maheu *et al.* (2003) used TOPEX/Poseidon altimetry over the Amazon, Lake Chad and Plata basin, respectively. Other authors such as Cauhopé *et al.* (2006), Frappart *et al.* (2006a), Frappart *et al.* (2006b) and Leon *et al.* (2006) utilized TOPEX/Poseidon and ERS/ENVISAT altimetry. These studies either made use of the GDR or estimated heights from the altimetric waveforms using conventional retracker schemes such as the ice-mode tracker (Ice-1) of ENVISAT.

The reliance on standard products or derivations using retrackers for ice/ocean surfaces places limitations on the geographical coverage to large lakes and rivers. For radar altimeters, the echoes are strongly affected by topography which may cause the altimeter to lose lock

* Correspondence to: S. J. Birkinshaw, School of Civil Engineering and Geosciences, Newcastle University, Newcastle NE1 7RU, UK.
E-mail: s.j.birkinshaw@ncl.ac.uk

resulting in data outages. Alternatively, the altimeter may return an echo from a water surface off-nadir giving rise to large errors in the range. The complexity of the reflecting surface will result in waveform echoes that differ from the single peak of an oceanographic return. Meaningful results over smaller bodies of waters and in areas of more difficult terrain can be recovered from the multi-peaked returns by utilizing a series of retracking schemes applied to the altimetric waveforms even when the standard retrackers fail to yield results (Berry *et al.*, 2005).

The altimetric water level measurements can be considered as a space borne virtual gauge providing discrete measurements at the repeat cycle of the satellite ground track (10-day TOPEX/Poseidon and Jason; 35-day ERS-2 and ENVISAT). An empirical rating curve based on either mathematical formulae or on measured stage and discharge data is used to convert the stage to discharge. With observed data, the rating curve is typically developed from measurements in low and medium flow conditions with the highest discharge values obtained by extending the rating curve by extrapolation. Spatially, rating curves are site specific owing to changing geometry but with possible temporal effects owing to vegetation changes, human intervention and changing channel geometry associated with transport and erosion of sediment. Kouraev *et al.* (2004) and Zakharova *et al.* (2006) produced rating curves using the altimetry water level measurements and the measured discharge data. This enabled discharge estimates to be made at times when *in situ* stage measurements were not available. Bjerklie *et al.* (2003) investigated alternatives to rating curves based on *in situ* data. Their approach utilized remotely sensed data to measure hydraulic variables from space and to derive discharge based on multiple regression analyses of discharge measurements. Statistically based models showed agreement with *in situ* data with accuracy within 50% for two thirds of the time.

In this study, we use altimetric stage data along the Mekong. The Mekong River basin is the sixth largest in the world in terms of discharge (*ca* 450 km^3/ year) and the 11th largest in terms of length (*ca* 4800 km). It rises on the Tibetan Plateau and flows into the South China Sea after passing through China (21% of drainage area, Burma (3%), Thailand (23%), Laos (25%), Cambodia (20%) and Vietnam (8%). The climate is dominated by the southwest monsoon between mid-May and early October leading to a seasonal rise in May and peak in September or October and the lowest levels in March and April. A major component of the dry season flows (up to 30%) is from snow melt in the upper basin (Mekong River Commission, 2005).

This study focusses on the Lower Mekong Basin, downstream of the northern Burma/Laos border, which contains 76% of the catchment area. Historical stage and discharge data are available at over 20 sites in the Lower Mekong Basin in Cambodia, Laos, Thailand and Vietnam (http://www.mrcmekong.org/).

Various hydrological models have been applied to the Mekong. Kite (2001) applied the semi-distributed SLURP hydrological model to the Mekong basin using publicly available data sets. The study focussed on generating flow to and from the Tonle Sap Lake for fisheries interests. Yang and Musiake (2003) applied a spatially distributed hydrological model that included sub-grid parameterizations of runoff generation mechanisms based on hillslope scale morphology, soil and land-use. Hapuarachchi *et al.* (2008) simulated the Mekong catchment using the grid-based distributed Yamanashi hydrological model (YHyM). They analysed the seasonal variations of climatic and hydrological characteristics of the basin (soil moisture, ground water saturation deficit, runoff, precipitation and evapotranspiration) for 1980–2000. Ishidaira *et al.* (2008) also used the YHyM model but examined the evolution of vegetation cover in the 21st century and its estimated impact on river discharge in the Mekong River basin. Where appropriate, this study makes use of the variable infiltration capacity (VIC) model (Liang *et al.*, 1994). Specifically, we use the lateral inflows along a section of the Mekong from an existing calibrated VIC model (Costa-Cabral *et al.*, 2008). The gauge data are subsequently employed to estimate discharge at a site some distance away.

This study aims to validate the discharge derived from the altimetric stage under the premise that *in situ* measured stage and discharge data are available at some other location along the river; a reasonable assumption for most large rivers. Without loss of generality, the site of the altimetric data is taken as downstream of the location of the *in situ* measured stage and discharge data. Two possible scenarios in which altimetric stage data is used to improve the accuracy of discharge estimates are considered. Firstly, the downstream site is at the location of a decommissioned gauging station. In this case there will be some historical information relating stage to discharge. This scenario is pertinent given that availability of global discharge data has decreased significantly since the mid-1980s (Nijssen *et al.*, 2001). The second scenario considers that altimetry is available at the downstream site that has never been gauged. In this more challenging case there is no rating curve from historical data, but it is assumed that the basic channel morphology is known, for example, from satellite imagery such as SAR. Since, the points chosen in the analyses are over 400 km apart the VIC model is used to provide a measure of the inflow along the intervening reach.

Our methodology differs from previous studies in two important ways. Firstly, the altimetry data are used to improve a daily time series of discharge for the predicted flow. Previous analyses have only produced point measurements that correspond with the timing of the satellite pass. Secondly, use is made of the method developed by Moramarco and Singh (2001) and Moramarco *et al.* (2005) where the downstream discharge at a site is predicted using the upstream discharge and the cross-sectional areas of the two sites.

ALTIMETRY DATA

Altimetric stage for the Mekong was derived using the retracking methodology detailed in Berry *et al.* (1997), Berry (2002) and Berry *et al.* (2005) based on the 20 Hz ERS-2 and 18 Hz ENVISAT altimetric waveforms. Initial results over the Amazon basin showed that even over the principal rivers in this network, the majority of echo shapes returned from the water surface which do not correspond to those obtained over the open ocean, but can be retracked using an expert system approach (Berry *et al.*, 2005). Because land is a relatively poor reflector of Ku-band energy compared with inland water the response from the water target frequently dominates the altimeter return. Complex echo shapes are still returned from land/water composite surfaces and where components other than the inland water response are significant. Each waveform is independently analysed; echoes containing complex shapes (generally resulting from a combination of land and water response or the presence of bright off-nadir reflectors contaminating the nadir response) have been filtered out prior to height determination and a suite of retrackers configured for the different waveform shapes are used to retrack each waveform to obtain the best range to surface estimate. The accuracy obtained when retracking non-Brown model waveforms is variable. For a simple quasi-specular echo extremely high accuracy may be obtained (Laxon, 1994). However, for more diffuse echoes the expected accuracy is in the range 2–10 cm. For more complex echoes the accuracy is lower. Having retained only simple waveform shapes the echoes are sorted into one of four categories; ocean like, flat patch and two categories of quasi-specular waveforms. Each waveform is then retracked by the algorithm designed for that echo shape. Retrackers for these waveform types are widely published in the literature (Wingham *et al.*, 1986; Laxon, 1994; Benveniste *et al.*, 2002).

It is emphasized that for effective retracking of echoes from inland water, it is essential that the retracker utilized for each waveform be configured to derive a mean range to surface for that waveform shape. Otherwise, offsets in the derived heights will be observed between echoes retracked by different algorithms, as may easily be confirmed by comparing heights over inland water derived from the four retrackers utilized in the ENVISAT SGDR product (Benveniste *et al.*, 2002). Altimeter heights that pass the quality checks are combined to provide a single stage measurement for the river crossing. As the along-track displacement between consecutive waveforms is approximately 350 m the retracker generally provided a single height although multiple heights per crossing were recovered on occasions. For two heights, a simple average was taken with a two-sigma filter and then averaging utilized for three or more measurements.

The accuracy of the altimetric stage is satellite dependent, primarily because the ENVISAT RA-2 was operated in high precision (ocean) mode over the majority of these targets, changing mode dynamically in response to assessment of its effectiveness in capturing the returned echoes, whereas the ERS-2 RA was placed in a less precise mode (ice mode) over all land surfaces. The practical implication is that, where good waveforms are successfully retrieved by the RA-2, higher vertical precision can be obtained; the drawback is that the 'ocean mode' is less tolerant to changing surface responses and topographic variation. As the bins of the ice-mode waveform tracker are four times larger than that of the ocean mode the height estimates from ERS-2 may individually be less precise than those from ENVISAT; however, more waveforms may be successfully acquired by ERS-2 because the dynamic mode-switching algorithms onboard ENVISAT only changes mode after four successive waveforms have not been properly captured, which can result in a significant loss of data over these river targets. Another significant factor is the quality of the returned echoes. ERS-2 returned very noisy echoes, a consequence of a limitation in the onboard waveform averaging process in which 50 individual echoes are averaged together to produce one output waveform which is telemetered to ground. In contrast, the ENVISAT RA-2 has an exceptionally good instrument, with almost no instrument noise apparent (Berry *et al.*, 2007) and where 100 individual echoes are averaged to form the telemetered output; the superb quality of these data assists in accurate retracking and hence precise surface height retrieval.

With both ERS-2 and ENVISAT following the same ground track within a 35-day repeat cycle, stage measurements are potentially available at the same river crossing every 35 days. Outages in the time series occur when no valid waveforms have been captured by the instrument during the satellite overpass or the retracking methodology fails to produce meaningful results. The different performance of the trackers onboard ERS-2 and ENVISAT with contrasting acquisition characteristics and the variation within the nominally repeating ground tracks accounts for the small differences in the mean geographic locations of the crossing points in Table I between ERS-2 and ENVISAT. Figure 1 and Table I show there are two different satellite passes close to Nakhon Phanom (NP) (104·8 °E, 17·4 °N) on days 16 and 33 of the 35-day repeat cycle, yielding data every 17 or 18 days. NP is near a crossover point of the ground track at the intersection of the ground tracks from an ascending pass and a descending pass.

COMPARISONS OF OBSERVED STAGE AND ALTIMETRY DATA

Time series of stage and discharge data from gauges along the Mekong were provided by the Mekong River Commission (http://www.mrcmekong.org/). Altimetry data are available from ERS-2 (1995–2003) and ENVISAT (2002–2008). The locations at which altimetry data have been extracted are shown in Figure 1 and some of these are in close proximity to the gauges allowing comparisons to be undertaken at six locations (Table I and Figure 1).

Table I. Mean locations of observed stage and ERS-2 (1995–2003) and ENVISAT (2002–2008) altimetry measurements and spherical Earth distance between gauge and altimetric data. River widths are for a typical dry season flow. MSL is the mean sea level

|	Latitude (°N)	Longitude (°E)	Base datum (m above MSL)	Distance from sea (km)	Distance to gauge (km)	River width (m)
Kompong Cham	11·909	105·388	−0·93	410		1700
ERS2(11·9n105·2e)	11·9372	105·2673	7·93		13·5	
ENVI(11·9n105·2e)	11·9381	102·2677	7·60		13·5	
Kratie	12·240	105·987	−1·08	545		1900
ERS2(12·2n105·9e)	12·2586	105·9140	11·80		8·2	
ENVI(12·2n105·9e)	12·2590	105·9134	10·91		8·3	
NP	17·398	104·803	130·96	1217		670
ERS2(17·5n104·7e)	17·5281	104·6995	137·89		18·2	
ERS2(17·5n104·6e)	17·5396	104·6889	138·62		19·9	
ENVI(17·5n104·7e)	17·5288	104·6982	138·32		18·3	
Paksane	18·372	103·667	142·13	1395		470
ERS2(18·3n103·8e)	18·3488	103·7855	148·93		12·8	
Vientiane	17·928	102·620	158·04	1580		460
ERS2(17·8n102·6e)	17·8371	102·6044	163·41		10·3	
ENVI(17·8n102·6e)	17·8374	102·6040	161·55		10·2	
Luang Prabang	19·892	102·137	267·19	2010		400
ENVI(20·0n101·9e)	20·0275	101·9496	285·62		24·7	
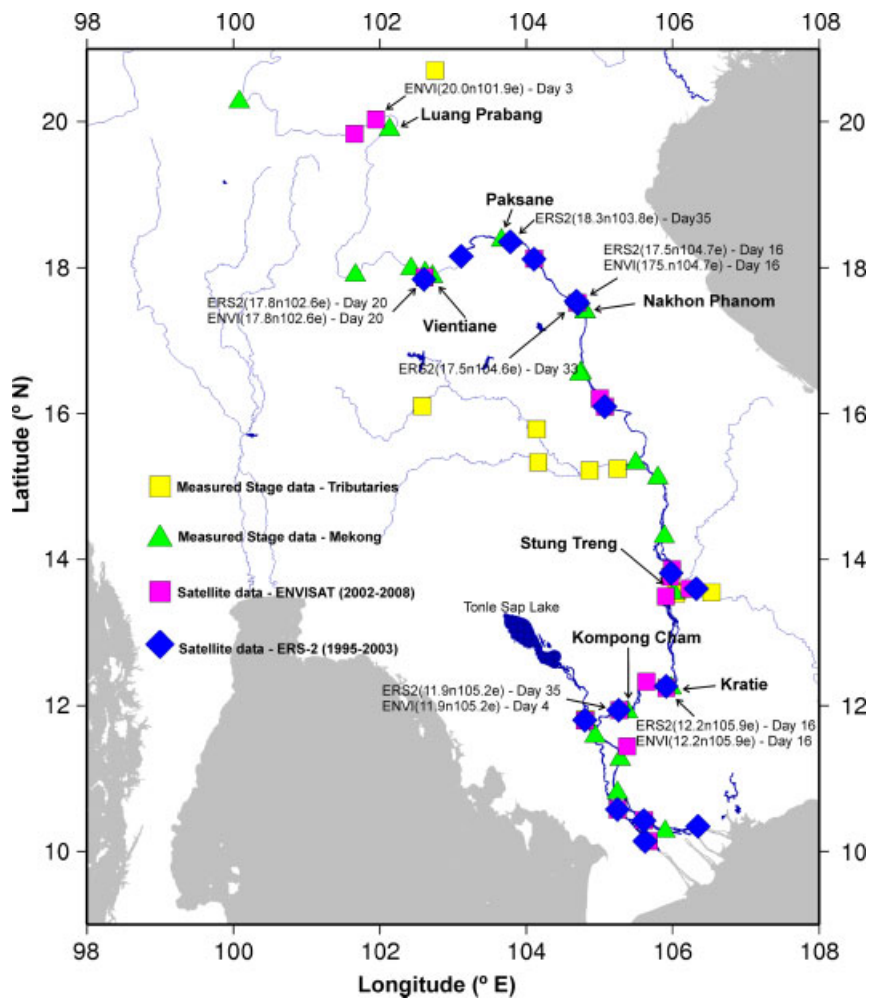
Figure 1. Available observed stage and altimetry data. Satellite altimetry data are obtained every 35 days, with the day and location of pass indicated. River network obtained from CIA database embedded in GMT (Wessel and Smith, 2009) programme
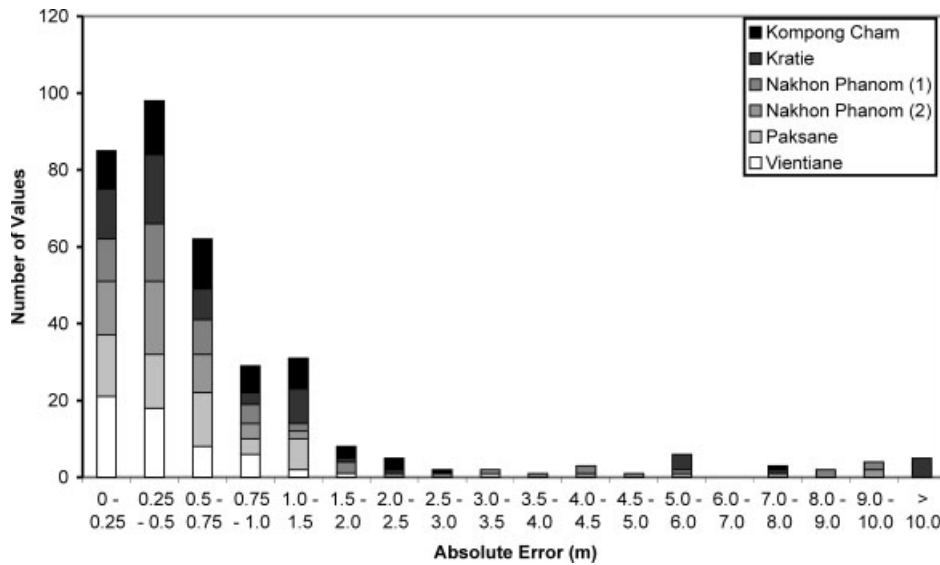
Figure 2. Histogram of errors between the ERS-2 altimetry data and the *in situ* stage data. There are two different satellite passes near NP

Kompong Cham, located upstream of the Tonle Sap Lake confluence, is the most southerly (downstream) location at which a comparison has been made. The river becomes affected by tidal influences around 50 km downstream of Kompong Cham. In upstream order from Kompong Cham the other gauged locations considered are Kratie, NP, Paksane, Vientiane and Luang Prabang.

The measured stage and altimetry data can be up to 30 km apart. Thus, the observed river stage measurements, o^t, at time t and the corresponding altimetry data, a^t, provide water levels to different data. Table I shows, for example, that the observed base datum for NP is 130·96 m above MSL, compared with 137·89 m and 138·62 m for ERS-2 and 138·32 for ENVISAT. The higher value for the satellite data is due to the crossing point being approximately 10 km upstream of the gauge observations, whereas the two ERS-2 data relate to the two separate ERS-2 crossings. For all locations, the satellite data were adjusted to a common datum. To allow direct comparison, the altimetry measurements have been subsequently adjusted by adding an offset, Z, derived by minimizing the absolute error (AE) between the observed and altimetry levels at concurrent times:

$$AE = \sum |o^t - (a^t + Z)| \qquad (1)$$

The corrected stage, h^t, are then

$$h^t = a^t + Z \qquad (2)$$

Accuracy of altimetry data

A number of the altimetry data points are found to be subject to significant error. For example, towards the end of the dry season on 7 May 1999 the corrected stage at NP is 10·39 m, whereas the measured stage is 0·83−an error of 9·56 m. In this case, it is possible that the satellite may be sensing irrigated land at the edge of the river. Figure 2 shows the discrepancies between the ERS-2 data and *in situ* gauge data for six satellite crossings. It can

be seen that most errors are less than 0·5 m. There are however, a substantial number of errors between 0·5 and 2 m. Beyond 2 m there are a small number of erroneous values which do not reduce in frequency as the error increases, with five values greater than 10 m. These large errors probably result from inaccuracies in locating the river particularly as some locations have islands/sand banks. Since, the satellite river crossing is only fixed to within ±1 km or so cross-track, substantial variability in the water/land target may be experienced for the same location.

In order to remove such large errors (i.e. those where it is not measuring the water level) a rejection criterion of 2 m is proposed, in the first instance for analysis of reliability using *in situ* data and later in order to develop a procedure for removing such outliers in the absence of validation data. Following this procedure, separate root mean square error (RMSE) values for ERS-2 and ENVISAT are presented in Table II. At all sites used for altimetry stage to gauge comparisons the RMSE difference is in the range 0·44−0·76 m on excluding Luang Prabang. At that location, the comparison was made between measurements about 30 km apart. Comparisons of the gauge and altimetry data show the altimetry data has much greater range suggesting the RMSE is due to different cross-sectional geometry at the gauge and altimeter locations. This site is not considered representative of the altimeter stage capability. Table II shows that the ENVISAT retracked altimeter heights are superior to those of ERS-2 at all locations. The ENVISAT altimeter has a minimum RMSE of 0·44 m at Vientiane and NP and a maximum of 0·65 m at Kratie. The ERS-2 has an RMSE which ranges from 0·46 m at Vientiane up to 0·76 m at Kompong Cham. Utilizing the measured stage−discharge relationship (Equation (4)) an RMSE of 0·44 m equates to a 7·2% error in the discharge during the wet season (for typical stage = 10 m).

Figure 1 shows other possible coincident gauge and satellite crossing locations particularly close to Stung

Table II. RMSE for the comparison between altimetry and measured stage data. Rejection criteria—error >2 m

	RMSE (m) ERS-2 (1995–2003)	Data points used (original number of points)	RMSE (m) ENVISAT (2002–2008)	Data points used (original number of points)
Kompong Cham	0·76	71(78)	0·57	34(34)
Kratie	0·70	69(81)	0·65	26(29)
NP	0·66,0·49	60(74),66(73)	0·44	26(31)
Paksane	0·72	73(75)		
Vientiane	0·46	62(62)	0·44	33(37)
Luang Prabang			1·24	16(25)

Treng. Here, ENVISAT provided data from three crossings at distances 13 km to the south and 24 km and 35 km to the north of the gauge as the river changes direction with respect to the satellite ground track. However, only the last crossing at distance 35 km from the gauge provided a meaningful comparison. This point was also the only crossing with ERS-2 data but was inconclusive as the comparison identified a large number of outliers. The other two crossings showed significant differences between high and low flow compared with the gauge—again suggesting very different channel geometries. This site illustrates the difficulty of extracting altimetric stage values even with retracked waveforms.

We note here that the RMSE values of Table II are higher than the 0·30 m found for TOPEX/Poseidon (T/P) by Cauhopé *et al.* (2006) for worldwide rivers and the 0·20 m for ERS-2 and 0·15 m for ENVISAT found by Frappart *et al.* (2006a) on the Amazon. There are several reasons for this related to the different locations and to the data analysis strategies. In particular, Frappart *et al.* (2006b) compared their altimetric virtual gauge time series against two gauges in the Lower Mekong with differences between *in situ* and altimetry stage levels of 0·23 m for ERS-2/ENVISAT at Moc Hoa and 0·15 m at Kompong Luong on the Tonle Lake for T/P. For both these delta and lake locations the width of the water level is considerably greater and the seasonal amplitude a factor of at least two lower than the upstream sites used in our study. The difference in terrain is emphasized by the fact that Frappart *et al.* (2006b) used altimetric heights from the ERS-2 GDR for ERS-2 and from the Ice-1 retracking scheme for ENVISAT. Neither approach would yield data from the upstream locations used in this study. The complexity of the terrain coupled with the larger amplitude compounds the analysis strategy.

Procedure for rejection of erroneous data

The above approach is useful for analysing the accuracy of the altimetry data with gauge data available. However, to be of general use the altimetry data needs to be used at sites where there is no *in situ* measured stage. For example, in this paper we are trying to make predictions of the discharge using altimetry data in isolation. Two possible methods were considered for identifying and rejecting erroneous data. The first method considers a single altimetry site and rejects those points outside the normal annual cycle of stage. However, this method is unsatisfactory as the start of the wet season can vary by up to 1 month. The second method considers all the contemporaneous altimetry data together and rejects those points outside set confidence bounds. This method will be considered in detail with the following procedure:

- Select all the crossings upstream of the Tonle Sap confluence (10 for ERS-2 or 12 for ENVISAT);
- Scale the data from each crossing so that the 10th percentile falls on 0 m and the 90th percentile on 10 m;
- For each point select data 30 days before and after and calculate the 99% confidence limits using Student's *t*-test;
- Widen the confidence limits by 1 m at either side;
- Select the point furthest outside the confidence limit and remove it;
- Recalculate the confidence limits and reject the next point furthest outside the confidence limit;
- Successively recalculate the confidence limits and remove points until all remaining points are contained.

Figure 3 shows the procedure for ERS-2 with data from ten gauges providing 734 points in total for the whole time period. During the procedure 118 points were rejected leaving 616. The ±1 m margin added/subtracted to the confidence limits is somewhat arbitrary but allows for the typical errors found in the altimetry data in the previous section. The data for both ERS-2 crossings and the ENVISAT crossing near NP are shown in Figure 4. In general the method works satisfactorily, but with some exceptions. For example, the data point on 12 July 2005 is accepted but with an error of 4·25 m. There is a rapid increase in stage at the start of the wet season resulting in wide confidence limits and acceptance of this point. In contrast, the data point on 8 September 2000 is rejected when it is in fact valid (error = 0·64 m). This is a secondary peak in the wet season and there are insufficient data in the altimetry datasets (of the 10 ERS-2 datasets used here) for this peak to be inside the confidence bounds. The RMSE from this method can be seen in Table III. The RMSE values are generally slightly higher using this rejection criterion than that based on the measured stage data. However, at NP the RMSE has increased significantly from 0·44 to 1·01 for the ENVISAT data (Tables II and III) as two bad data points on 27 July 2004 and 12 July 2005 (Figure 3) are now included. For ENVISAT at Vientiane and Kompong Cham, the RMSE is now
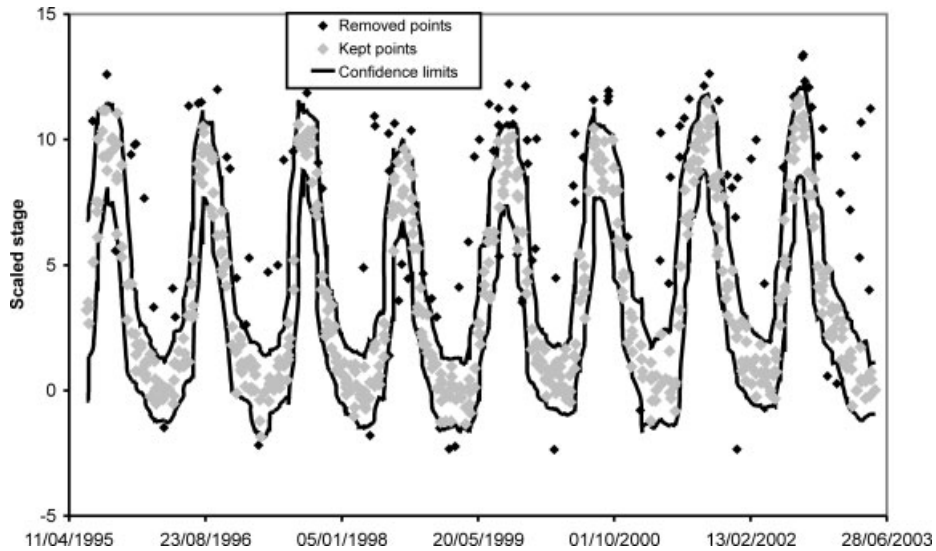
Figure 3. Rejected points, accepted points and confidence bounds for the ERS-2 altimetry data
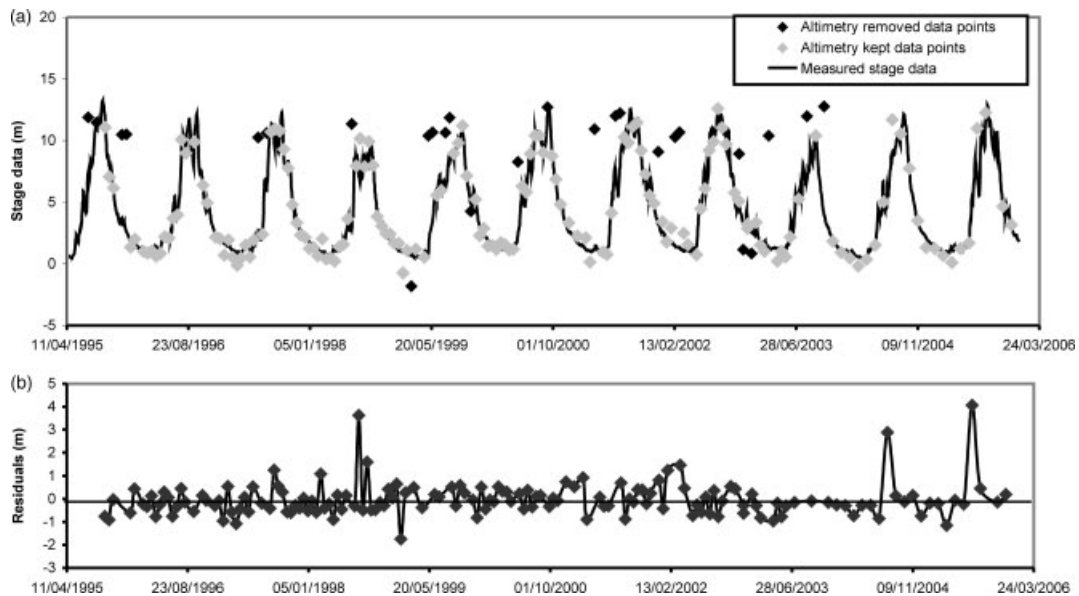

Figure 4. Comparison of observed stage data (NP) and altimetry data (ERS-2 and ENVISAT) (a) altimetry water levels, (b) residuals (showing only kept data points)

Table III. RMSE for the comparison between altimetry and measured stage data. Rejection criteria based on confidence bounds using all the altimetry data

	RMSE (m) ERS-2	Data points used (original number of points)	RMSE (m) ENVISAT	Data points used (original number of points)
Kompong Cham	0·96	60 (78)	0·54	30 (34)
Kratie	0·80	66 (81)	0·75	27 (29)
NP	0·77,0·49	58 (74),66 (73)	1·01	24 (31)
Paksane	0·76	68 (75)		
Vientiane	0·47	55 (62)	0·41	29 (37)
Luang Prabang			1·99	22 (25)

slightly lower than before (Tables II and III), as some of the data points with errors around 1–2 m are now excluded. Excluding Luang Prabang, the number of data points now accepted is 84% compared to 90% during the previous procedure. Luang Prabang is again a special case. More points are accepted during this procedure resulting in an increase in the RMSE from 1·24 m to 1·99 m. The data points accepted at NP using this method were used in the next two sections for predicting daily discharge.

USE OF ALTIMETRY DATA TO IMPROVE THE ESTIMATE OF DISCHARGE AT A DECOMMISSIONED SITE

NP is located about 400 km downstream of Vientiane. NP has two passes of ERS-2 altimetry in close proximity (Figure 1). Both sites have stage and discharge data from 1961 to 2000. Table IV shows the mean monthly discharge at Vientiane and NP for the years 1960–1995. The discharge at NP was considerably higher than at Vientiane, particularly during periods of high flows. For example, in August the mean discharge at NP was some 70% larger than the mean discharge at Vientiane, indicating significant lateral inflow along the reach.

Table IV. Mean discharge data (1960–1995) at Vientiane and NP and the ratio between the two

| | Mean discharge (m³/s) | | Ratio |
	Vientiane	NP	
January	1781·56	2365·23	1·33
February	1378·45	1837·18	1·33
March	1177·64	1523·30	1·29
April	1192·66	1474·39	1·24
May	1679·70	2248·18	1·34
June	3470·06	6583·66	1·90
July	6890·69	12 584·82	1·83
August	11 136·01	18 819·53	1·69
September	10 774·54	17 824·65	1·65
October	6934·60	10 021·30	1·45
November	4323·34	5354·09	1·24
December	2612·88	3326·87	1·27

For the purpose of this analysis, it was assumed that the NP Station was decommissioned at the end of 1995, that the Vientiane Station continued to the end of 2000 and there were no other gauging data in between. A linear regression model (based on 1960–1995 data) relating the discharge at Vientiane and the discharge at NP was developed. This model was used to produce a prediction of the discharge time series at NP for the period 1996–2000. The altimetry data is then used to improve this prediction, making use of the measured stage–discharge relationship from 1994 to 1995. The predictions are then compared against the measured discharge data to assess how much the altimetry data has improved the predictions.

Decommissioned site with a linear regression model without altimetry data

A linear regression model was used to estimate the discharge at NP from the discharge at Vientiane (V). The best fit using 1960–1995 data was

$$Q_{NP-LR}{}^t = 1 \cdot 602 \, Q_V^t \quad (3)$$

where Q_{NP-LR} (m³/s) is the discharge at NP estimated using the linear regression model, Q_V (m³/s) the measured discharge at Vientiane and t the time in days. Predicted discharges compared to the actual measured discharges are plotted in Figure 5. There is generally a good correspondence with a Nash–Sutcliffe r^2 efficiency of 0·884 (Nash and Sutcliffe, 1970). Some major differences are noted, particularly, in September 1996 when the peak was not captured, owing to the major lateral inflows between NP and Vientiane.
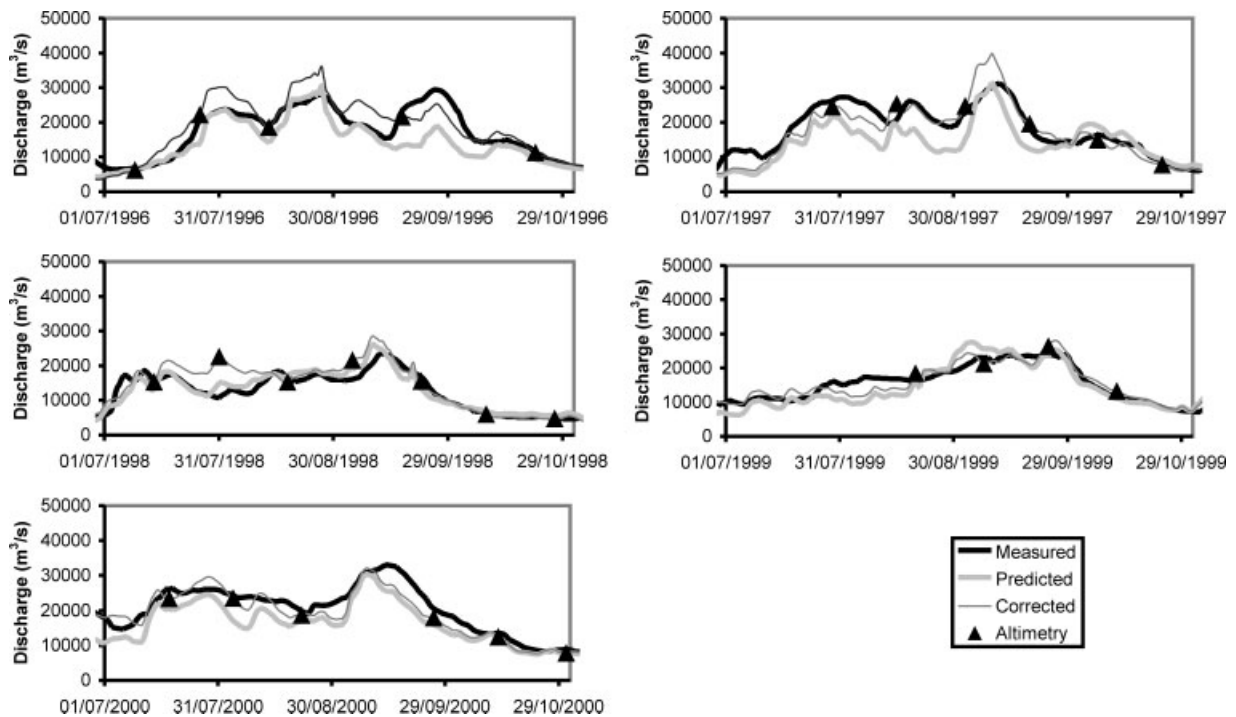

Figure 5. Decommissioned site scenario: measured, predicted (using Vientiane flows with a linear regression model), corrected prediction (using altimetry data) and altimetry data points at NP 1996–2000. Altimetry data points are from the measured stage height converted to discharge using the measured stage–discharge relationship (Equation (4))
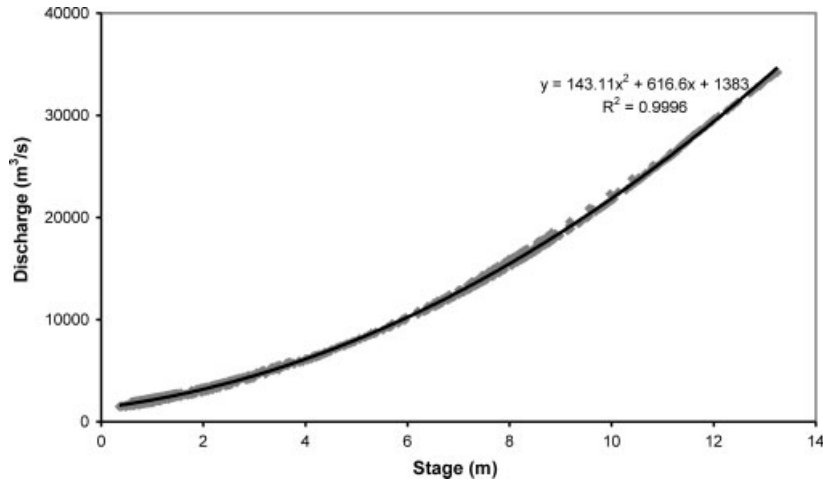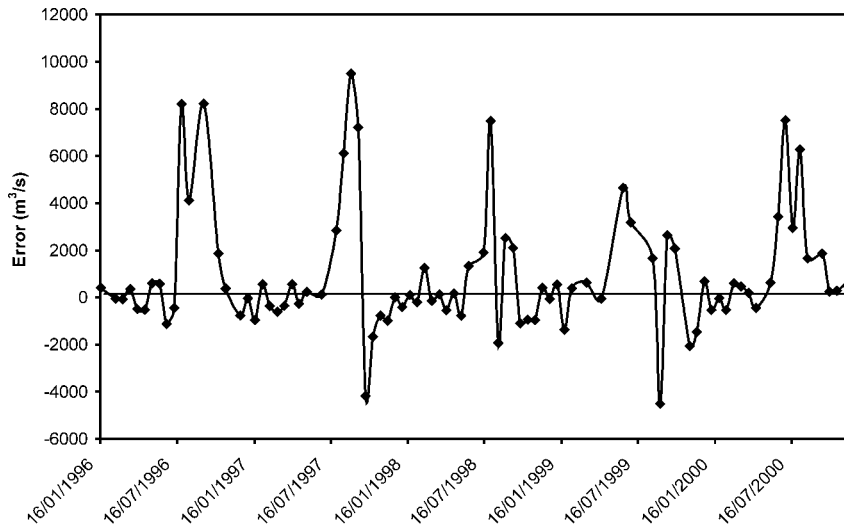
Figure 6. 1994–1995 stage–discharge relationship at NP

Figure 7. Errors (m³/s) between altimetry discharge and predicted linear regression discharge at NP for each altimetry point

Two other methods were tested. The Muskingum method such as that proposed by Franchini and Lamberti (1994) was found to perform less well. The transfer function approach (Young, 2002) produced similar predicted discharges to the linear regression approach. However, the best fitting model was that discharge at NP depended on the discharge in the previous day and the current discharge at Vientiane (rather than discharge at Vientiane several days earlier as might be expected from consideration of travel time for flood waves).

Decommissioned site with a linear regression model with altimetry data

Figure 6 shows the measured stage–discharge relationship for NP for the period 1994–1995. As stated previously, it is assumed here that these data were available, that is the gauge was decommissioned at the end of 1995. Using this relationship, the altimetry data were directly converted to discharge (i.e. without the need for information from Vientiane) via

$$Q_{\mathrm{NP-SAT}}{}^{t} = 143{\cdot}11 \quad (h_{\mathrm{NP-SAT}}{}^{t})^{2} + 616{\cdot}6$$

$$h_{\mathrm{NP-SAT}}{}^{t} + 1383 \qquad (4)$$

where $Q_{\mathrm{NP-SAT}}$ is the estimated altimetry discharge at NP and $h_{\mathrm{NP-SAT}}$ is the altimetry stage at NP.

The altimetry data from the two satellite passes available at NP (converted to discharge) are also plotted in Figure 5. The flows obtained using the altimetry data are considered the best estimates at the decommissioned site. As seen in Table III, the RMSE of the altimetry levels at this site was 0·63 m (average of the two satellite passes) which equates to around a 10% error in discharge in the wet season. Assuming that these values represent 'truth', an error function for the linear regression model of Equation (3) was defined by

$$\varepsilon_{\mathrm{NP-LR}}{}^{t} = Q_{\mathrm{NP-SAT}}{}^{t} - Q_{\mathrm{NP-LR}}{}^{t} \qquad (5)$$

Figure 7 shows the error between the altimetry discharge and predicted linear regression discharge on using Equation (5). Adjacent values have an autocorrelation of 0·41. Thus, a positive value on one altimetry data will generally gives a positive value the next pass. Linear interpolation was used to model the error function

between adjacent values. For example, if the altimetry gives data at times t and $t + 17$ then the error at time $t + 4$ is

$$\varepsilon_{\mathrm{NP-LR}}^{t+4} = \varepsilon_{\mathrm{NP-LR}}^{t} + 4 \times (\varepsilon_{\mathrm{NP-LR}}^{t} - \varepsilon_{\mathrm{NP-LR}}^{t+17})/17 \tag{6}$$

Using Equations (5) and (6), the corrected linear regression model at NP is:

$$Q'_{\mathrm{NP-LR}}{}^{t} = Q_{\mathrm{NP-LR}}{}^{t} + \varepsilon_{\mathrm{NP-LR}}{}^{t} \tag{7}$$

The corrected discharge using the revised linear regression model is plotted in Figure 5. By design, the corrected discharge is exactly the same as the discharge derived from altimetry data and historical rating curve at the time of the altimetry pass. However, as the time increases from the previous overpass there is greater reliance on the linear regression model. Clearly, there is some improvement using the altimetry data, particularly, in September 1996. The altimetry data were measured on 17 September 1996 prior to the peak and there is a large difference (8219 m^3/s) between the altimetry discharge and the predicted linear regression discharge (Figure 7). This difference is used to correct the linear regression data at times near this epoch. However, the corrections on 26 July 1996 and 13 August 1996 now mean that the discharge in the first two peaks in 1996 is over-estimated. Overall, using the altimetry data the Nash−Sutcliffe r^2 value for the 1996−2000 period has improved from 0·884 to 0·935.

USING ALTIMETRY DATA TO IMPROVE THE ESTIMATE OF DISCHARGE AT AN UNGAUGED SITE

In this section, we consider that NP is ungauged. The discharge at Vientiane and lateral inflows from a hydrological model between Vientiane and NP are used to produce a prediction of the discharge time series at NP. The altimetry data is subsequently used to improve this prediction, assuming that river channel cross-sections are known at Vientiane and NP. As previously, the predictions are then compared against the measured discharge data to assess how much the altimetry data has improved the predictions.

The VIC model

The VIC model (Liang *et al*., 1994) is a semi-distributed grid-based macro-scale hydrologic model which represents explicitly the effects of vegetation, topography and soils on the exchange of moisture and energy between land and atmosphere. Costa-Cabral *et al.* (2008) have previously applied the VIC model to the Mekong and it is this dataset that is used here. A model grid resolution of 1/12° (approximately 10 × 10 km) of latitude and longitude was used. This choice was dictated by a compromise between the density of the *in situ* (primarily precipitation) data available to drive the model and the inherent spatial variability of land surface characteristics that the model is intended to represent. The VIC

model is used to provide a measure of lateral inflows between the upstream gauged site and the downstream ungauged site.

Ungauged site using the VIC model without altimetry data

In this case it was assumed that the discharge data at NP was unknown and that the estimated discharge at NP depends on the sum of the flows at Vientiane and the VIC lateral inflows between Vientiane and NP. Use of the flows at Vientiane should consider modification owing to the attenuation of the peaks and the travel time to reach NP. However, tests using the Price formula (Price, 1973) found that the attenuation was less than 5% of the peak flow and, considering the inaccuracies in the VIC modelling, the attenuation was not taken into account.

Without access to gauge data the travel time from the upstream to the downstream site can be inferred from theory or statistical analyses. Döll *et al.* (2003) suggested a value of 1 m/s for the velocity of the water for a large number of the major rivers. However, the celerity of the flood wave is often around 1·5 times the value of the velocity (Chow *et al.*, 1988). Thus, assuming a value of 1·5 m/s during the wet season a 3-day time lag is inferred for sites about 400 km apart. Hence, the discharge at NP was taken to be equal to the discharge at Vientiane 3 days earlier complemented by the VIC lateral inflows between Vientiane and NP, namely,

$$Q_{\mathrm{NP-UG}}{}^{t} = Q_V^{t-3} + Q_{\mathrm{VIC}}^{t} \tag{8}$$

Before making use of the VIC data, it is informative to compare the VIC lateral inflows with the measured lateral inflows from the period 1979 to 1995. Measured lateral inflows between Vientiane and NP were calculated by using the measured discharges at the two sites. The inflows at time t were calculated as the discharge at NP at time t minus the discharge at Vientiane 3 days earlier (i.e. assuming the 3-day travel time), with analogous inflows from VIC. Figure 8 shows the VIC inflows were generally considerably smaller than the measured inflows. Table V shows the monthly ratio between measured inflows from 1979 to 1995 and the VIC inflows. With the exception of May, the measured lateral inflows are higher. This is a data sparse region with clear shortcomings in the quality of the rainfall data.

The predicted discharge (Equation (8)) compared with the observed data at NP can be seen in Figure 9 for the wet season in 1996−2000. As expected, the performance is worse than the method for a decommissioned site with a Nash−Sutcliffe r^2 efficiency of 0·823. Furthermore, this method considerably underestimates the flows owing to the corresponding underestimation of the lateral inflows from VIC (Table V).

Theoretical basis for developing a stage−discharge relationship

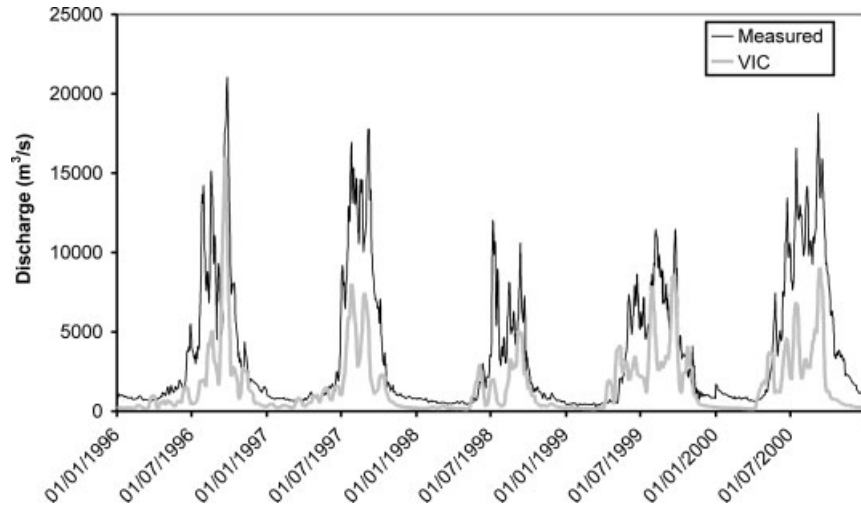The estimation of discharge for each measured altimetry stage data (and the development of an estimated

Figure 8. Difference in inflow (m³/s) between the Vientiane and NP gauging sites

Table V. Monthly ratios (1979–1995) of the measured lateral inflows between Vientiane and NP and the VIC lateral inflows along the same stretch of river

Month	Ratio
January	2·61
February	2·31
March	1·88
April	1·56
May	0·95
June	2·53
July	2·65
August	2·03
September	2·09
October	1·83
November	1·63
December	2·23

stage–discharge relationship) is based on the assumption that the upstream and downstream mean channel velocities are equal (Chiu, 1991). Leopold and Maddock (1953) found that channel velocities remain similar as the change in local channel slope is compensated for by the change in depth. With subscripts u and d referring to the upstream and downstream site, respectively and T_L the travel time from the upstream to downstream site, the velocity (V) at time t is,

$$V_d^t = V_u^{t-T_L} \qquad (9)$$

Using the cross-sections given in the Mekong River Commission website (http://www.mrcmekong.org/), the measured stage was converted to a cross-sectional area using basic geometry. For example, the cross-section for NP can be seen in Figure 10. For the three sites this gave cross-sectional areas (A) as a function of the stage data (h) as follows:

$$A_{LP} = 800 + 400h_{LP} + 5·4\,h_{LP}^2 \qquad (10)$$

$$A_V = 1930 + 460h_V + 7·5h_V^2 \qquad (11)$$

If $h_{NP} \leq 9$ $\qquad A_{NP} = 3510 + 670h_{NP} + 5h_{NP}^2$

If $h_{NP} > 9$ $\qquad A_{NP} = 9945 + 760(h_{NP} - 9)$
$$+ 58·3(h_{NP} - 9)^2 \qquad (12)$$

The constants of the quadratics are the area of the cross-section when the stage is zero that is it is the area under the water surface at minimum level. The linear term of the quadratics relate to the width of the river when the stage is zero. The power term of the quadratics relate to the increasing width of the river as the stage increases.

The mean flow velocity can be estimated by dividing the measured discharge by the areas of Equations (10)–(12). Figure 11 shows that plausible and similar values are obtained at the three locations. The velocity varies throughout the year with a value of around 0·5 m/s in the dry season and up to 2 m/s in the wet season. However, at any time the velocities at the three Mekong sites are very similar, revealing strong temporal correlations between the sites. The flow velocity at NP and at Vientiane 3 days earlier, are also in good agreement (Figure 12). The fitted line has gradient of 1·204 indicating that mean velocities are on average higher at NP than at Vientiane, which is consistent with theory for large rivers (Leopold and Maddock, 1953). This will affect the accuracy of the estimated stage–discharge relationship calculated later.

The sensitivity of Equations (10)–(12) to error can be inferred by considering a channel of width W, bank slope of 45° (cf. Figure 10), stage h above minimum water level and A_{min} the cross-sectional when the stage is zero. Denoting δh to be the error in h etc then

$$\delta A \approx W\,\delta h + h\delta W/2 + \delta A_{min}. \qquad (13)$$

On taking $W = 670$ m, $h = 10$ m as pertinent to NP the error in the cross-sectional area for $\delta h = 0·60$ m and $\delta W = 20$ m is ≈ 600 m² with the contribution from δh being double that of δW. δA_{min} is more difficult to quantify and we have taken $\delta A_{min} = 200$ m² which equates to about a 6% error in the dry season cross-sectional area at NP. On using Equation (12), the cross-sectional area error estimate of 800 m² is about 7·5% of the area
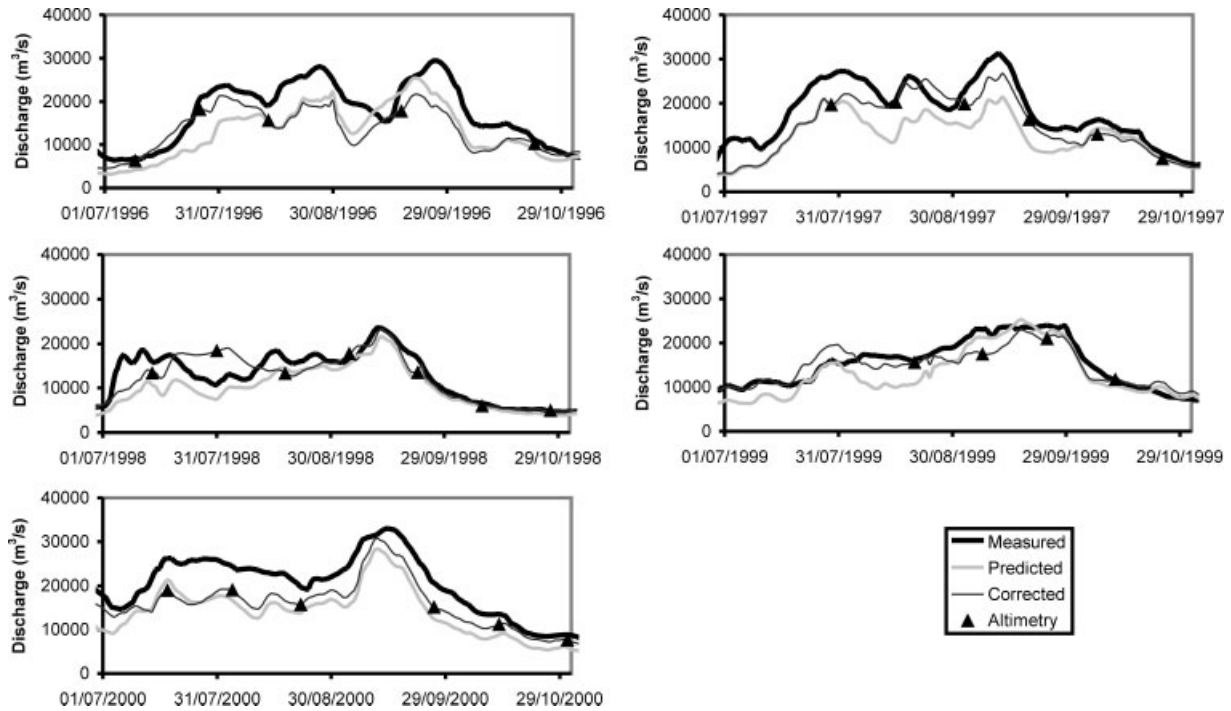
Figure 9. Ungauged site scenario: measured, predicted (using Vientiane flows and VIC), corrected prediction (using altimetry data) and altimetry data points at NP 1996–2000. Altimetry data points are from the measured height converted to discharge using the estimated stage–discharge relationship (Equation (15))
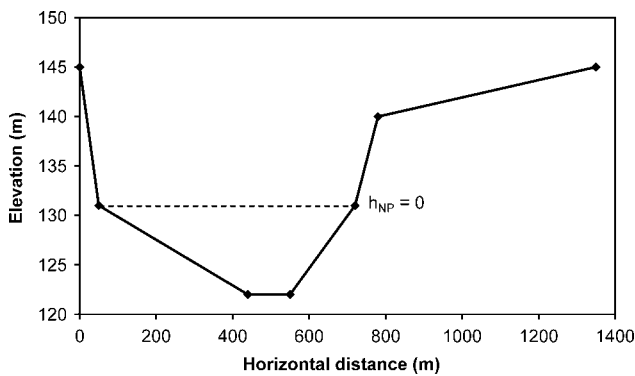

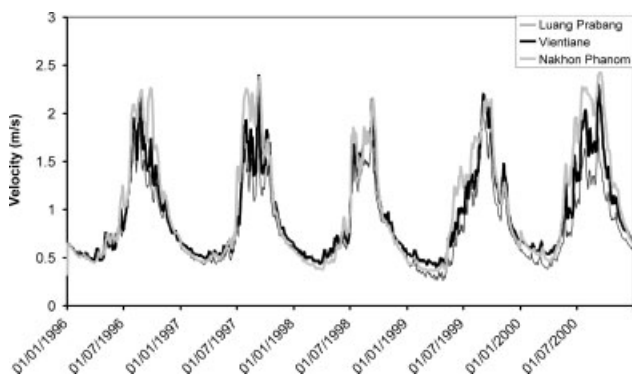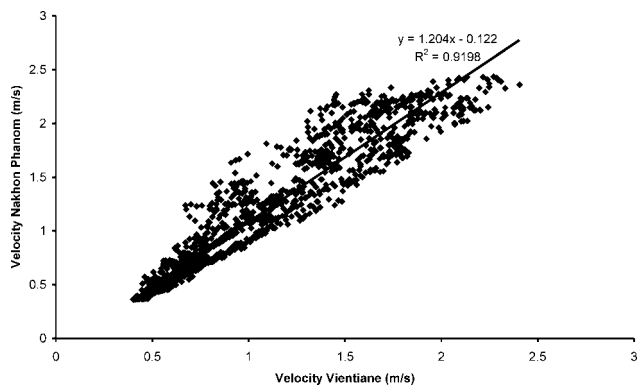Figure 10. River cross-section at NP

Figure 12. Scatter plot showing mean channel velocity at NP and mean channel velocity at Vientiane 3 days earlier

Ungauged site using the VIC model and altimetry data

To make use of the altimetry data to improve the discharge predictions a stage–discharge relationship is needed. For the decommissioned scenario this was straightforward as there was an existing stage–discharge relationship. However, in the ungauged scenario a rating curve needs to be developed. To do this the discharge at NP for each altimetry data point is estimated using the discharge at Vientiane and the cross-sectional areas at Vientiane and NP (Equations (11) and (12)). This is based on the formula in Equation (9) but now considers the discharge (Q) and cross-sectional areas (A).

$$Q'^t_{NP-SAT} = (A^t_{NP}/A^{t-3}_V)Q^{t-3}_V \qquad (14)$$

where $Q'_{NP-SAT}{}^t$ is the altimeter estimated discharge at NP, $Q_V{}^{t-3}$ the measured discharge at Vientiane 3 days

Figure 11. Mean channel velocity at Luang Prabang, Vientiane and NP

(10 763 m²) during the wet season. We note here that the error in width approximately corresponds to the synthetic aperture radar resolution on ERS-2 while the error in stage was the RMSE value seen with ERS-2.
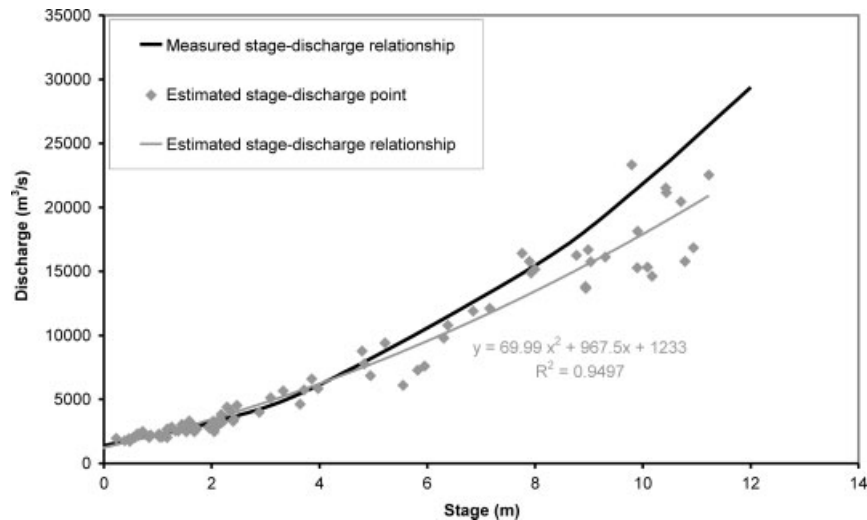
Figure 13. Estimated stage–discharge relationship at NP

earlier and $A_{\text{NP}}{}^{t}$, $A_{V}{}^{t}$ the cross-sectional areas at the sites. This formula is very similar to the one developed by Moramarco and Singh (2001) and Moramarco *et al.* (2005). However, their formula is simplified here as there is insufficient data at NP to fit the two extra parameters used in their study.

Using the above method the estimated discharge at NP is compared with the altimetry stage data in order to produce an estimated stage–discharge relationship. Figure 13 shows that this estimation is approximately correct. The main difference compared with the actual stage–discharge relationship is that the estimated discharges will be smaller than the actual discharges for large flows. The estimated stage–discharge relationship

$$Q'^{t}_{\text{NP-SAT}} = 69 \cdot 99(h^{t}_{\text{NP-SAT}})^{2} + 967 \cdot 5 h^{t}_{\text{NP-SAT}} + 1233 \quad (15)$$

is used to convert the measured altimetry stage data to discharge data.

An error function can be found between the predicted and the estimated altimetry discharges

$$\varepsilon^{t}_{\text{NP-UG}} = Q'^{t}_{\text{NP-SAT}} - Q^{t}_{\text{NP-UG}} \quad (16)$$

where $Q_{\text{NP-UG}}$ is the predicted discharge at the ungauged NP site (Equaion (8)), $Q'_{\text{NP-SAT}}$ the estimated altimetry discharge (using the estimated stage–discharge relationship, Equation (15)) and $\varepsilon_{\text{NP-UG}}$ the estimated error at the ungauged NP site. As before linear interpolation yields the correction each day.

The corrected discharges can be seen in Figure 9 for the wet seasons in 1996–2000. This shows an improved match using the altimetry data. For example, for the event at the end of July 1996 the corrected discharge is now closer to the actual discharge as the corrected discharge must pass through the altimetry point of 26 July 1996 which is close to the measured discharge. The corrected discharges are generally lower than measured discharges as they must pass through the estimated altimetry points which are generally too low due to errors in the estimated stage–discharge relationship. Overall, the Nash–Sutcliffe

r^{2} efficiency has increased from 0·823 to 0·893 on using the altimetry data.

DISCUSSION AND CONCLUSIONS

Comparisons of retracked altimetry and observed stage measurements have been carried out at six sites along the Mekong. Rejecting those altimetry data points with errors greater than 2 m gives RMSE for the ERS-2 (ENVISAT) altimetry data of 0·76 m (0·57 m) at Kompong Cham, 0·70 m (0·65 m) at Kratie, 0·66 m and 0·49 m (0·44 m) at NP, 0·72 m at Paksane and 0·46 m (0·44 m) at Vientiane. The large error of 1·24 m at Luang Prabang is thought to be due to the different channel geometries at the altimetry and gauge sites. The comparisons show that the accuracy of the altimetric stage is satellite dependent. ENVISAT was operating in its high precision ocean mode over the majority of these targets, changing mode dynamically in response to assessment of its effectiveness in capturing the returned echoes, whereas ERS-2 was in a less precise mode over all land surfaces. In consequence, where good waveforms are successfully retrieved by ENVISAT a higher vertical precision can be obtained however, the 'ocean mode' is less tolerant to changing surface responses and topographic variation and less passes are tracked. Altimetry provides stage but for many applications it is the corresponding discharge that is of importance. In terms of discharge, an RMSE of 0·44 m equates to a 7·2% error during the wet season.

Altimetry data will be of most use at sites where existing observed stage is not available so a different error procedure, based solely on the altimetry data, was needed. This was achieved by using all the altimetry data contemporaneous within 30 days of the data point and rejecting points outside a 99% confidence bound determined using the Student's *t*-test. Generally robust results have been demonstrated with roughly equal numbers of false rejections and acceptances.

To investigate the potential of altimetry for improvement of the quality of discharge measurements two

Table VI. Summary of Nash−Sutcliffe r^2 efficiency values and RMSE for the comparison of daily measured and predicted discharges at NP

	r^2 without altimetry data	r^2 with altimetry data	RMSE without altimetry data (m³/s)	RMSE with altimetry data (m³/s)
Decommissioned scenario	0·884	0·935	2650	1986
Ungauged scenario	0·823	0·893	3271	2546

sites were considered, Vientiane upstream and NP downstream. Two scenarios were tested making use of the accepted data points found using the confidence bounds. Firstly, that the stage at NP was decommissioned in 1995 and, secondly, that NP has never been gauged. In the first scenario, predictions were made for the discharge between 1996 and 2000 using standard methods and using the altimetry data. These were compared against the actual measured data observations. The altimetry data improved the Nash−Sutcliffe r^2 value from 0·884 to 0·929. In the second scenario, predictions were made for the discharge between 1996 and 2000 using the upstream discharge at Vientiane and the VIC hydrological model for lateral inflows. The analysis shows the potential of using the method of Moramarco *et al*. (2005) to produce a stage−discharge relationship. In essence, by assuming that the velocities are the same at the upstream and downstream sites (with time lag depending on the travel time) and that the upstream discharge and the cross-sectional areas at the upstream and downstream sites are known, then the downstream discharge can be derived. Enhancements to this method (not used here) may take into account the expected larger velocities downstream (Leopold and Maddock, 1953). The altimetry data improved the Nash−Sutcliffe r^2 value from 0·823 to 0·893. A summary of the improvements can be seen in Table VI.

In this study, upstream discharge is clearly paramount to accurate predictions downstream. The former can be determined from a gauge or a macro-scale hydrological model. Macro-scale hydrological models such as VIC are critically dependent on availability and quality of precipitation time series, often available only from satellites such as TRMM. The use of the modelled discharge upstream and the linear regression approach used in this study can only modify the downstream discharge relative to that upstream with commensurate error if the upstream discharge is erroneous. This deficiency is overcome if a time series of discharge is available from an upstream site. In this case, the study shows that there is clear potential for the use of altimetry data to provide accurate estimates of discharge downstream. The methodology utilizes the upstream and downstream cross-sectional areas; the altimetry providing the height variation with *in situ* or remote sensing data providing the river geomorphology. In particular, remote sensing data (e.g. Bjerklie *et al*., 2003) can be used to supply a time series of river width, which, with altimetry, yields the time-varying cross-sectional area at the sub-satellite points. Further studies utilizing remote sensing data are planned to quantify this approach.

This study has clearly shown that satellite altimetry data can, in certain cases, improve estimates of the daily discharge time series. The Mekong is a well instrumented catchment and hence provides an excellent opportunity to validate the techniques. However, the real potential of the techniques presented here will be for poorly instrumented sites where there are few *in situ* measurements and such studies are planned.

REFERENCES

Alsdorf DE. 2003. Water storage of the central Amazon floodplain measured with GIS and remote sensing imagery. *Ann. Assoc. Am. Geogr.* **93**(1): 55−66.
Alsdorf DE, Rodrıguez E, Lettenmaier DP. 2007. Measuring surface water from space. *Rev. Geophys.* **45**: RG2002, DOI:10.1029/2006RG000197.
Alsdorf DE, Smith LC, Melack JM. 2001. Amazon foodplain water level changes measured with interferometric SIR-C radar. *IEEE Trans. Geosci. Remote Sensing* **39**(2): 423−431.
Bates PD, Wilson MD, Horritt MS, Mason DC, Holden N, Currie A. 2006. Reach scale floodplain inundation dynamics observed using airborne synthetic aperture radar imagery: data analysis and modelling. *J. Hydrol.* **328**: 306−318.
Benveniste J, *et al*. 2002. *ENVISAT RA-2/MWR Product Handbook, Issue 1·2*, PO-TN-ESR-RA-0050, European Space Agency: Frascati, Italy.
Berry PAM. 2002. A new technique for global river and lake height monitoring using satellite altimeter data. *Int. J. Hydropower Dams* **9**(6): 52−54.
Berry PAM, Freeman JA, Rogers C, Benveniste J. 2007. Global analysis of ENVISAT RA-2 burst mode echo sequences. *IEEE Geosci. Remote Sens. Lett.* **45**(9): 2869−2874, DOI:10.1109/TGRS.2007.902280.
Berry PAM, Garlick JD, Freeman JA, Mathers EL. 2005. Global in—land water monitoring from multi-mission altimetry. *Geophys. Res. Lett.* **32**: L16401, DOI:10.1029/2005GL022814.
Berry PAM, Jasper A, Bracke H. 1997. *Retracking ERS-1 altimeter waveforms over land for topographic height determination: an expert system approach*, European Space Agency Specifications Publ.: ESA SP-414, 403−408.
Birkett CM, Mertes LAK, Dunne T, Costa MH, Jasinski MJ. 2002. Surface water dynamics in the Amazon Basin: application of satellite radar altimetry. *J. Geophys. Res.* **107**(D20): 8059−8080.
Bjerklie DM, Dingman SL, Vörösmarty CJ, Bolster CH, Congalton RG. 2003. Evaluating the potential for measuring river discharge from space. *J. Hydrol.* **278**: 17−38.
Cauhopé M, Gennero MC, DoMinh K, Cretaux JF, Berge-Nguyen M, Cazenave A, Seyler F. 2006. *Worldwide validation of satellite

altimetry-based water level time series. EGU06-A-02342, HS52, EGU General Assembly 2006, 02–07 April 2006 Wien (Austria).

Chiu CL. 1991. Application of the entropy concept in open channel flow. *J. Hydraulic Eng.* **117**: 615–628.

Chow VT, Maidment DR, Mayes LW. 1988. *Applied Hydrology*. McGraw-Hill: New York; 572 p.

Coe MT, Birkett CM. 2004. Calculation of river discharge and prediction of lake height from satellite radar altimetry: example for the Lake Chad basin. *Water Resour. Res.* **40**: W10205, DOI:10.1029/2003WR002543.

Costa-Cabral MC, Richey JE, Goteti G, Lettenmaier DP, Feldkotter C, Snidvongs A. 2008. Landscape structure and use, climate, and water movement in the Mekong River basin. *Hydrol. Processes* **22**: 1731–1746, DOI:10.1002/hyp.6740.

Döll P, Kaspar F, Lehner B. 2003. A global hydrological model for deriving water availability indicators: model tuning and validation. *J. Hydrol.* **270**: 105–134.

Franchini M, Lamberti P. 1994. A flood routing muskingum type simulation and forecasting model based on level data alone. *Water Resour. Res.* **30**: 2183–2196.

Frappart F, Calmant S, Cauhopé M, Seyler F, Cazenave A. 2006a. Preliminary results of ENVISAT RA-2 derived water levels validation over the Amazon basin. *Remote Sens. Environ.* **100**: 252–264.

Frappart F, Do Minh K, L'Hermitte J, Cazenave A, Ramillien G, Le Toan T, Mognard-Campbell N. 2006b. Water volume change in the lower Mekong from satellite altimetry and imagery data. *Geophys. J. Int.* **167**(2): 570–584.

Hapuarachchi HAP, Takeuchi K, Zhou MC, Kiem AS, Georgievski M, Magome J, Ishidaira H. 2008. Investigation of the Mekong River basin hydrology for 1980–2000 using the YHyM. *Hydrol. Processes* **22**: 1246–1256.

Ishidaira H, Ishikawa Y, Funada S, Takeuchi K. 2008. Estimating the evolution of vegetation cover and its hydrological impact in the Mekong River basin in the 21st century. *Hydrol. Processes* **22**: 1395–1405.

Kouraev AV, Zakharovab EA, Samainc O, Mognard NM, Cazenave A. 2004. Ob'River discharge from TOPEX/Poseidon satellite altimetry (1992–2002). *Remote Sens. Environ.* **93**: 238–245.

Kite G. 2001. Modelling the Mekong: hydrological simulation for environmental impact studies. *J. Hydrol.* **253**: 1–13.

Laxon S. 1994. Sea ice altimeter processing scheme at the EODC. *Int. J. Remote Sensing* **5**: 915–924.

Leon JG, Calmant S, Seyler S, Bonnet M-P, Cauhopé M, Frappart F, Filizola N, Fraizy P. 2006. Rating curves and estimation of average water depth at the upper Negro River based on satellite altimeter data and modeled discharges. *J. Hydrol.* **328**: 481–496.

Leopold LB, Maddock T. 1953. *The hydraulic geometry of stream channels and some physiographic implications*. U. S. Geol. Survey Prof. Paper 262.

Liang X, Lettenmaier DP, Wood EF, Burges SJ. 1994. A simple hydrologically based model of land surface water and energy fluxes for general circulation models. *J. Geophys. Res.* **99**(D7): 14415–14428.

Maheu C, Cazenave A, Mechoso CR. 2003. Water level fuctuations in the Plata basin (South America) from Topex/Poseidon satellite altimetry. *Geophys. Res. Lett.* **30**(3): 1143–1146.

Mekong River Commission. 2005. *Overview of the Hydrology of the Mekong Basin*. Mekong River Commission, Vientiane, November 2005, 73 pp.

Moramarco T, Barbetta S, Melone F, Singh VP. 2005. Relating local stage and remote discharge with significant lateral inflow. *J. Hydrol. Eng.* **10**: 58–69.

Moramarco T, Singh VP. 2001. Simple method for relating local stage and remote discharge. *J. Hydrol. Eng.* **6**: 78–81.

Nash JE, Sutcliffe JV. 1970. River flow forecasting through conceptual models part I—A discussion of principles. *J. Hydrol.* **10**(3): 282–290.

Nijssen B, O'Donnell GM, Lettenmaier DP, Lohmann D, Wood EF. 2001. Predicting the discharge of global rivers. *J. Climate* **14**: 3307–3323.

Price RK. 1973. Flood routing method for British rivers. *Proc. Inst. Civ. Eng., Waters. Martime Engin.* **55**: 913–930.

Smith LC, Pavelsky TM. 2008. Estimation of river discharge, propagation speed, and hydraulic geometry from space: Lena River, Siberia. *Water Resour. Res.* **44**: W03427, DOI:10.1029/2007WR006133.

Vörösmarty CJ, Birkett C, Dingman L, Lettenmaier DP, Kim Y, Rodriguez E, Emmitt GD. 1999. *NASA Post-2002 Land Surface Hydrology Mission component for Surface Water Monitoring: HYDRASAT HYDRlogical Altimetry SATellite*. A report from the NASA Post-2002 Land Surface Hydrology Planning Workshop, Irvine, CA, 12–14.

Wessel P, Smith WHF. 2009. The Generic Mapping Tools (GMT) version 4.5.0 Technical Reference & Cookbook, SOEST/NOAA.

Wingham DJ, Rapley CG, Griffiths H. 1986. New techniques in satellite altimeter tracking systems. In Proceedings of IGARSS'86 Symposium, Zurich, 8–11 Sept. 1986, Ref. ESA SP-254 (1339–1344).

Yang D, Musiake K. 2003. A continental scale hydrological model using the distributed approach and its application to Asia. *Hydrol. Processes* **17**(14): 2855–2869.

Young PC. 2002. Advances in real-time flood forecasting. *Philos. Trans. Roy. Soc. Lond.* **360**: 1433–1450.

Zakharova EA, Kouraev AV, Cazenave A, Seyler F. 2006. Amazon River discharge estimated from the TOPEX/Poseidon altimetry. *C. R. Geoscience* **338**: 188–196.